Net Water Movement in Budd Inlet: Measurements and Conceptual Model

Curtis C. Ebbesmeyer and Carol A. Coomes
Evans-Hamilton, Inc.

Venkat S. Kolluru and John Eric Edinger
J.E. Edinger Associates, Inc.

Introduction

Previous oceanographic studies of Budd Inlet assumed a two-layered flow pattern typical of estuaries, i.e., the upper water layer flowing out of the inlet above a deeper, inflowing stratum (URS Corporation, 1986). We examined this assumption during a year-long field program to assess the effects of permitting additional effluent into the inlet from the Lacey-Olympia-Tumwater-Thurston County (LOTT) wastewater treatment plant. The field measurements and a three-dimensional (3-D) hydrodynamical model led to a new dynamical framework for the inlet's flow.

Budd Inlet's circulation was monitored along a number of east-west oriented transects (Figure 1). South of the BA transect, the inner inlet's northern boundary, the flow is largely controlled by gated discharges from Capitol Lake and large tidal ranges that daily expose extensive tide flats. North of the BA transect, the estuarine flows are primarily separated laterally rather than vertically, as shown later in this paper.

Physical Setting

Budd Inlet, Puget Sound's southernmost marine water body, composes 0.15% of the Sound's total volume at mean high water (MHW) (McLellan, 1954). Because the tide range generally increases with distance inland, the inlet's range is penultimate in Puget Sound (14.4 feet; 4.4 m). Table 1 lists selected physical characteristics of the inlet.

Table 1. Budd Inlet: selected physical characteristics.

	Non-Metric Units	Metric Units
Inlet length from mouth to head[1]	6.8 statute miles	10.9 km
Width at mouth[3]	0.99 statute miles	1,600 m
Fresh water input during November 1996 from:		
LOTT sewage treatment plant	11 mgd[2]	0.48 m^3/sec
Direct rainfall on inlet[4]	34 mgd	1.5 m^3/sec
Inlet net inflow along western shore[5]	6,875 mgd	300 m^3/sec
Capitol Lake (average)	350 mgd	15 m^3/sec
Capitol Lake (gates closed ~ 48% of time)	0	0
Capitol Lake (gates open ~ 52% of time)	672 mgd	30 m^3/sec
Tide range (diurnal[6])	14.4 feet	4.39 m
Inlet volume below mean higher high water (MHHW)	301,000,000 yd^3	230,000,000 m^3
Inlet water surface area at:		
mean high water (MHW)	8.8 square miles	22,680,000 m^2
mean lower low water (MLLW)	7.2 square miles	18,560,000 m^2
Mean inlet depth (volume/surface area)	30 feet	10 m
Flushing time (Inlet volume @ MHHW/inflow net transport)	7–11 days	600,000–950,000 sec

[1] From the Capitol Lake gates to the inlet Mouth (center of the line connecting Dofflemeyer and Cooper points);
[2] million gallons/day
[3] Line connecting Dofflemeyer and Cooper points;
[4] Rain falling on the inlet's surface area at MHW;
[5] Through the cross section near inlet mouth;
[6] Diurnal tidal range equals MHHW minus MLLW.

The Deschutes River empties into Capitol Lake which in turn discharges to the southern terminus of the inner inlet via control gates so as to maintain a nearly constant lake level (Davis et al., 1998). The long-term monthly average Deschutes discharge varies from a maximum during January of approximately 600 cfs (17.0 m^3/sec), to a minimum during August of 50 cfs (1.4 m^3/sec). Superposed on the seasonal swing are discharge pulses caused by periodically opening the gates. For several hours a day, the lake discharges as if it were a substantial river; for most of the day, however, it discharges no fresh water. During the extremely wet winter of 1996–1997, for example, discharge during gate openings often exceeded 100 m3/sec and reached 300 m^3/sec.

Methods

The inlet's flow was ascertained from field observations (water properties, currents) and a hydrodynamical model.

Water Properties

Temperature, salinity, density, and dissolved oxygen were measured versus depth using Seabird conductivity-temperature-pressure (depth) CTDs lowered from two vessels (models SBE 19 and 25 equipped with AFM modules and rosette water bottles). From September 1996 through September 1997 during 23 cruises each lasting a day, 27 locations along and across the inlet were sampled.

Current Meter Observations

Water flow was monitored with current meters moored for a year at three sites (Figure 1): sites 1 and 2, on the west and east sides of the BE transect, respectively, were taken as representative of the inlet's mouth; and site 3, on the west side of the BC transect in the central inlet. Currents also were measured for a month at several other sites (see Figure 1).

Two types of current meters were deployed: 1) Acoustic Doppler Profilers (ADPs; RDI broadband 300 kHz and Sontek 1500 kHz) placed on the bottom measured currents between a few meters of the sea surface and sea floor. Current speed and direction were averaged for two minutes every 15 minutes in 0.5 and 1 m depth intervals (bins) at sites 1–4. To filter out tidal variability, the observations within each depth bin were vector-averaged over one tidal day (24.84 hours) and 28 calendar days. 2) Aanderaa current meters were moored at fixed depths. Current speed was averaged during 15-minute intervals, at the end of which current direction was recorded.

Additional, more detailed, current measurements were made to examine the velocity structure across the inlet's mouth: 1) during 14–15 March 1997, an ADP was mounted over-the-side while the vessel (*R/V Reflux*) made 24 crossings of the BE transect; 2) during September 1997, two ADPs were deployed at sites 1 and 2 toward the west and east sides of the inlet, respectively, while three Aanderaas were moored at mid-channel.

Hydrodynamic Model

For comparison with the current measurements and water properties, the 3-D hydrodynamic and transport model known as GLLVHT (Edinger and Buchak, 1995) was programmed to compute water transport west and east of a north-south line approximately dividing the inlet in half (see Figure 1). Calculated water transport was averaged during 28-day intervals; these were then averaged during November 1996–January 1997.

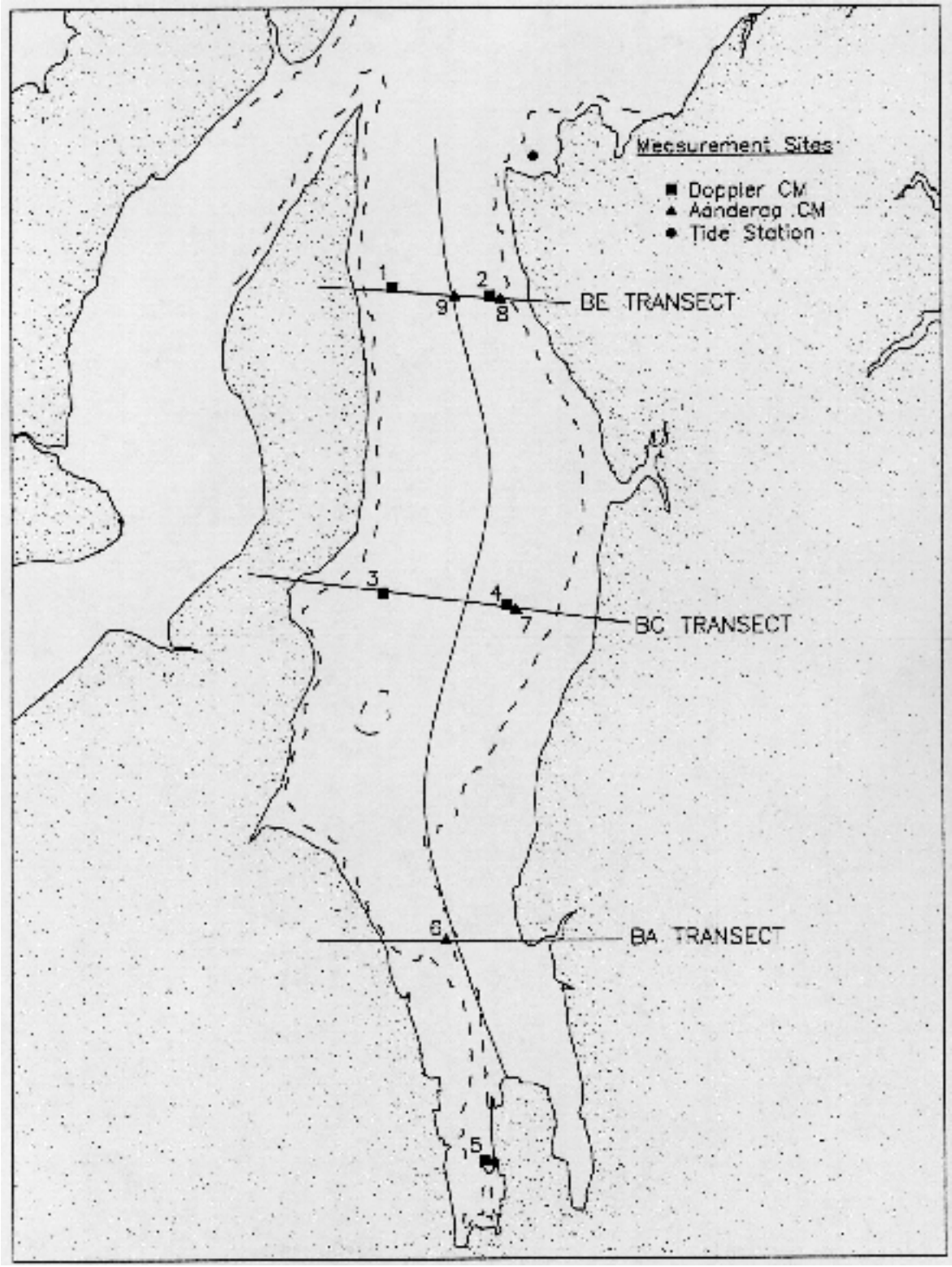

Figure 1. Locations of current meters and transects in Budd Inlet. Squares denote ADP current meters on the sea floor; triangles, Aanderaa current meter moorings; circles, water level recorders; transect lines, outer (BE), central (BC), inner (BA); dashed line, the 18-foot depth contour from bathymetric surveys. Net transports were computed west and east of the line down the center of the inlet.

Results: Water Properties

Water properties were contoured throughout the inlet in horizontal planes at constant depths, and across the inlet in vertical planes along the transects. The thousands of planes contoured showed similar water mass patterns throughout the year. For illustrative purposes, the depth plane nearest the sea surface (0.5 m) was chosen to trace the plume of fresh water from Capitol Lake (Figure 2). The BC transect was chosen to illustrate the cross-inlet structure, because four as opposed to three or fewer stations on the other transects were sampled along it (Figures 3 and 4).

In each season at 0.5-m depth, the contours of temperature, salinity, density, and oxygen were generally oriented north-south, indicating that Capitol Lake effluent traveled northward as a plume along the inlet's eastern shore. More saline Puget Sound water flowed southward along the western shore. Illustrative contours for spring (16 April 1997), show the freshwater plume as approximately 0.6 _C warmer, 2 ppt less saline, 1 sigma-t units less dense, and 1–2 mg/L more oxygenated than the water flowing southward along the western shore.

The separation line between the inflowing and outflowing currents was observed during July 1997, when operators drained Capitol Lake to perform annual maintenance (removal of undesirable plants). A few days afterward a rip line containing large amounts of plant material floating on the water surface was photographed. The line extended seven miles from Capitol Lake northward through the outer inlet. Comparison with the water property contours indicated that the plant debris traced the separation between the inflowing and outflowing currents.

Taken together, the 23 cruises spread over a year showed plumes of relatively low salinity water along the eastern shoreline in 70% of the density and 83% of the salinity contours in the 0.5-m depth plane. Furthermore, closed temperature and oxygen contours at 0.5 m revealed elevated levels in the central inlet indicative of a gyre. Closed contours were found in 22% of the temperature and 57% of the oxygen contours.

Contours across each transect almost always showed the plume as a lens along the eastern shore (Figures 3, 4). The salinity difference between the lowest values in the plume and the highest values in the Puget Sound water along the western shore is a fundamental estuarine parameter. Along the BC transect the difference varies from 6 ppt during fall and winter to 2–3 ppt during spring and summer. As the plume is both warmer and less saline than the source waters feeding the inlet, and since both temperature and salinity act to decrease density within the plume, the density contours mimic those of temperature and salinity.

In the cross-sectional contours, the oxygen concentrations are higher than in the source waters by 1–2 mg/L during fall and winter, a difference increasing to 3–6 mg/L during spring and summer. Note that the minimum oxygen concentrations occur approximately beneath the surface plume flowing northward along the eastern shore (Figure 4).

Regardless of water property, the inlet's water mass was separated laterally across the inlet, a structure reflected by the current measurements.

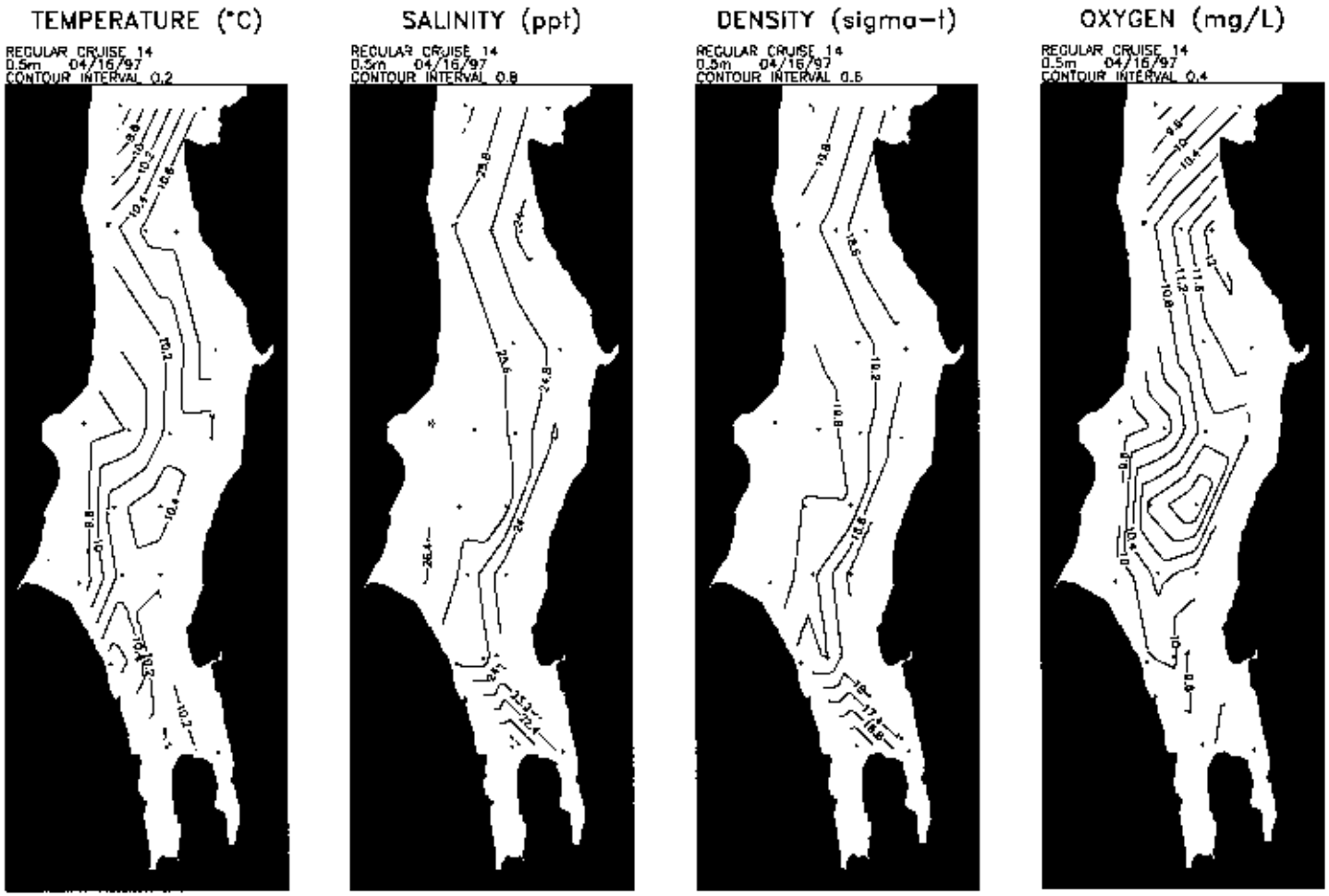

Figure 2. Spring (16 April 1997) near-surface (0.5 m) contours (from left to right): temperature, salinity, density, and dissolved oxygen. Dots indicate locations of CTD profiles. Note that the contour interval changes with season.

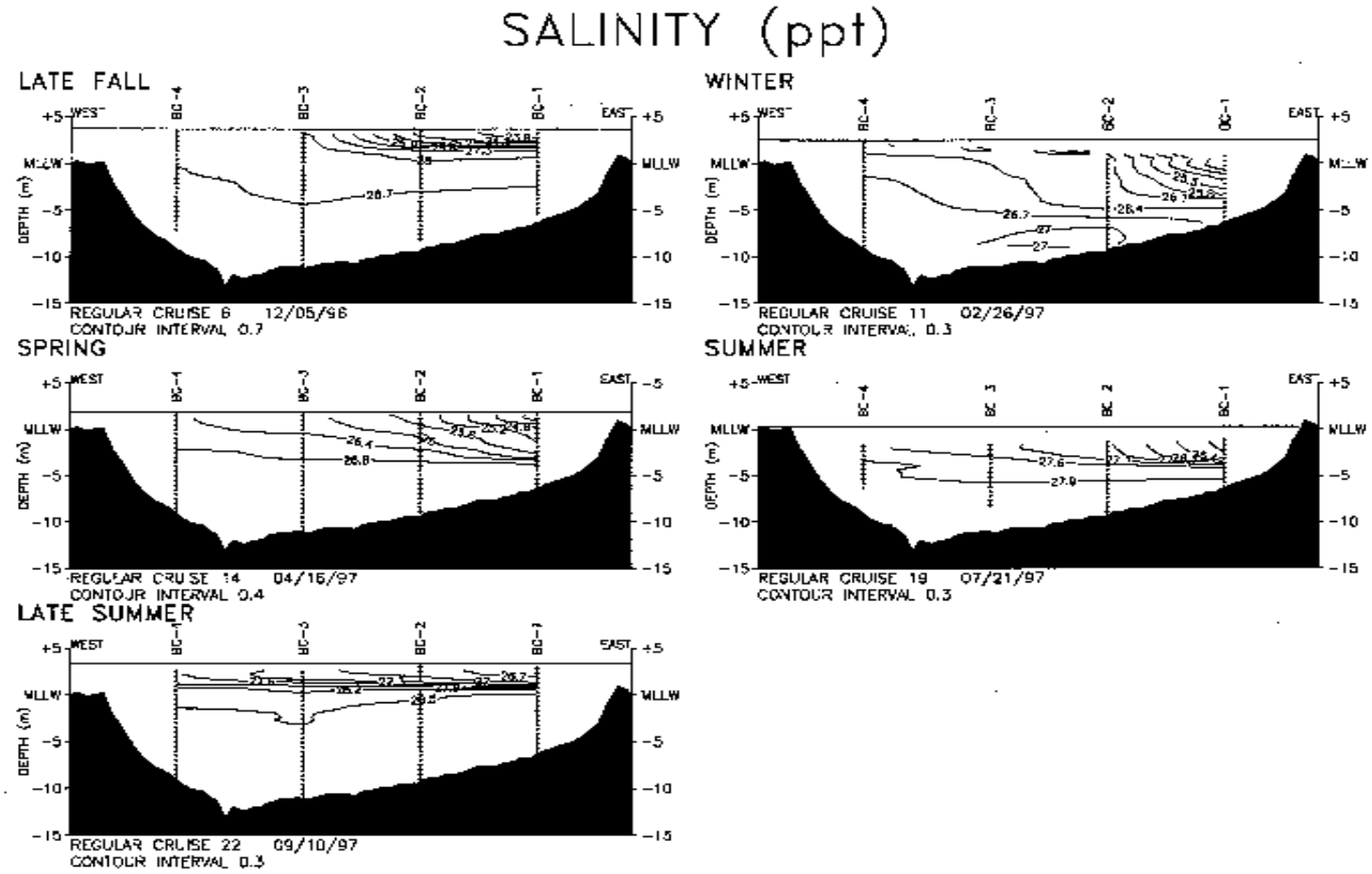

Figure 3. Seasonal salinity contours along the BC transect (left to right, top to bottom): Late Fall, 5 December 1996; Winter, 26 February 1997; Spring, 16 April 1997; Summer, 21 July 1997; Late Summer, 10 September 1997. Dots indicate CTD data. Note that the contour interval changes with season.

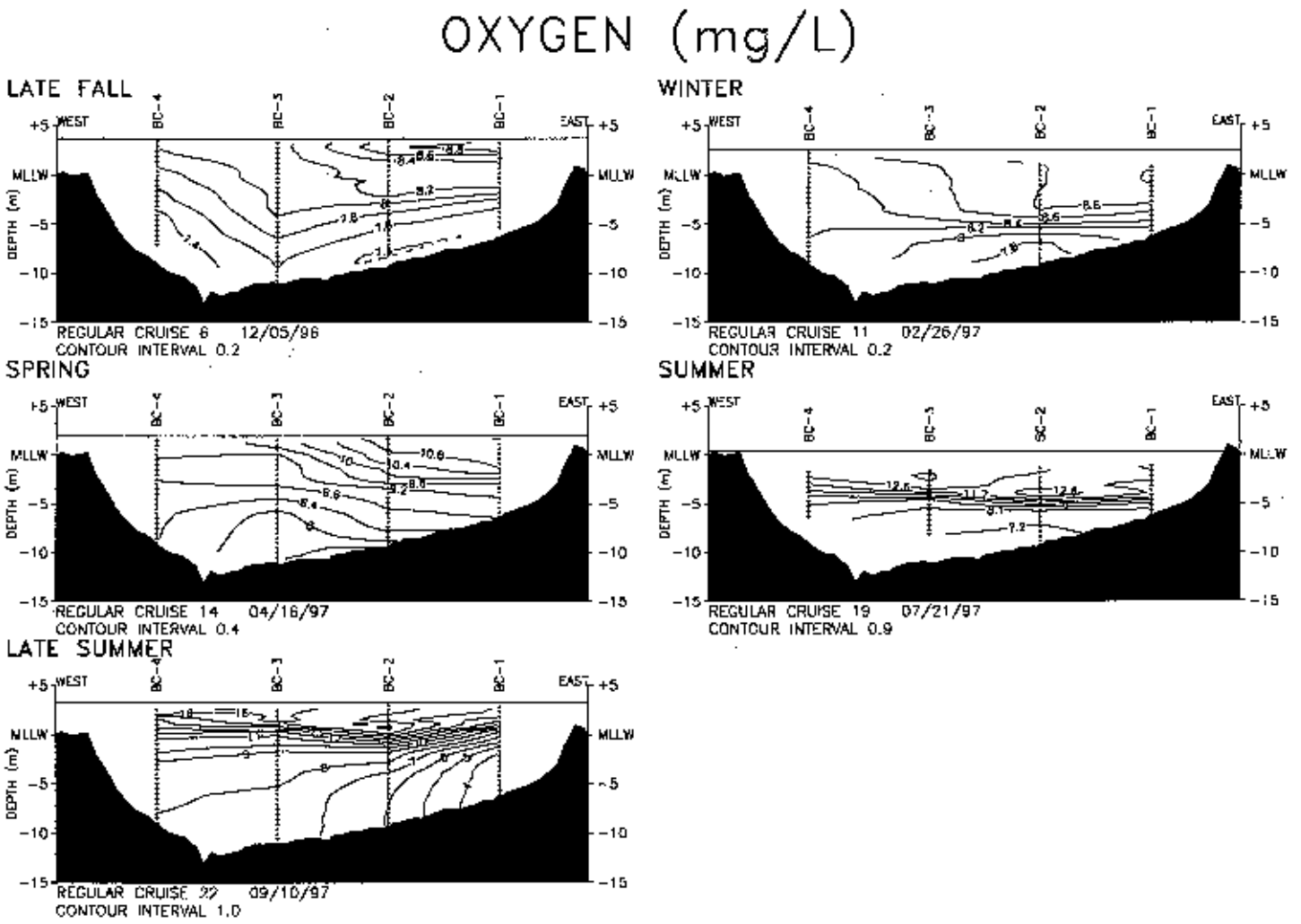

Figure 4. Seasonal dissolved oxygen contours along the BC transect (left to right, top to bottom): Late Fall, 5 December 1996; Winter, 26 February 1997; Spring, 16 April 1997; Summer, 21 July 1997; Late Summer, 10 September 1997. Dots indicate data. Note that the contour interval changes with season.

Results: Velocity Structure

To examine the current structure across the inlet's mouth, north-south current speed (V), as averaged for a tidal day and 28 calendar days, was contoured along the BE transect (Figure 5). Both sets of more detailed cross-inlet velocity measurements showed that the mean inflow and outflow are separated laterally by a line of no-net-motion (zero-speed contour) centered over the hump between the flood (west) and the ebb (east) tidal channels.

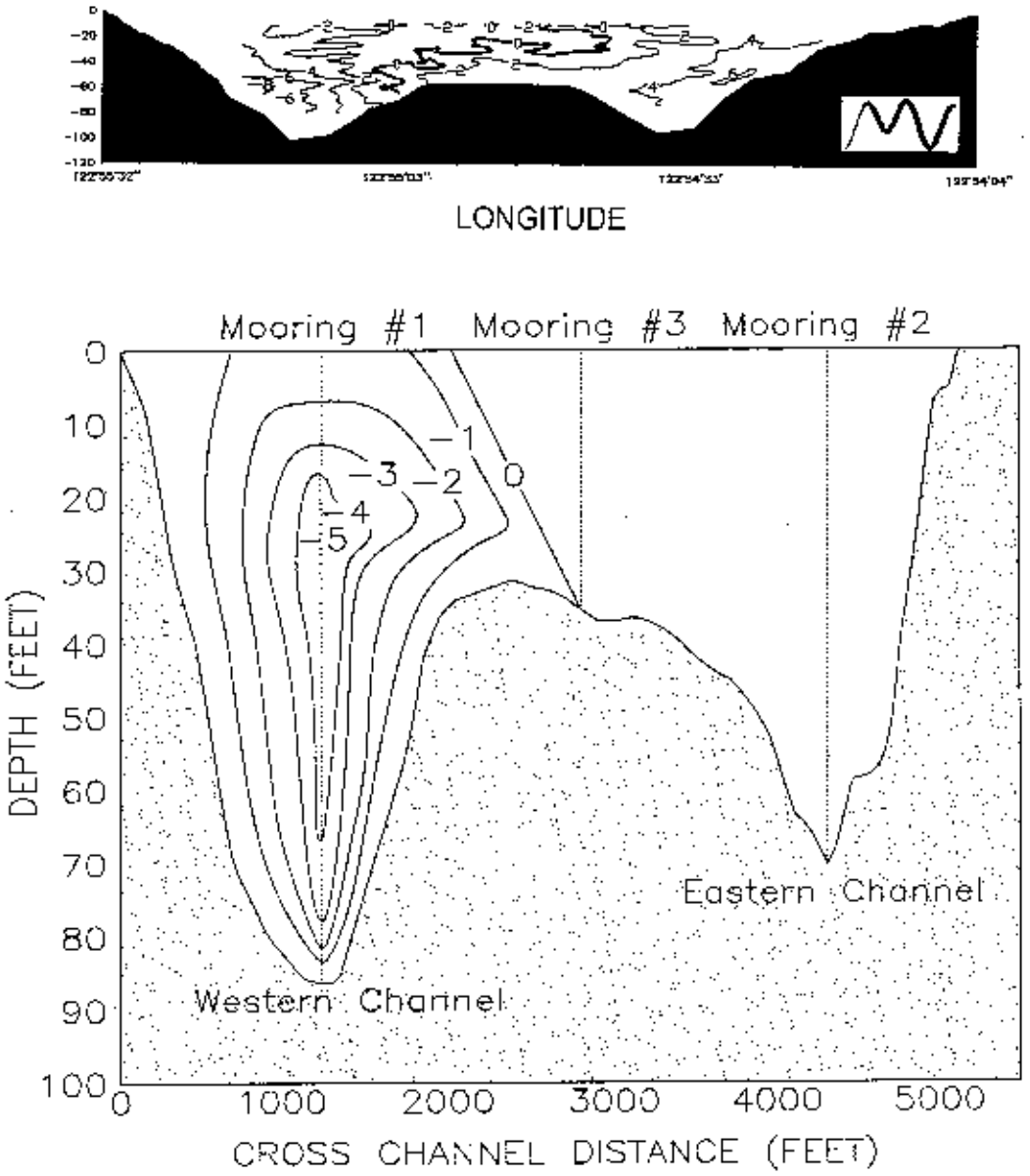

Figure 5. Current speed across Budd Inlet: detailed examination. The cross-channel structure of the average north-south currents was contoured with two kinds of averages (see Figure 1 for transect locations). Upper panel: 24 crossings of the BE transect with an ADP mounted over the side during a 25-hour survey during 14–15 March 1997, where the contour interval equals 2 cm/sec. Inset at lower right shows the tide over which the transects were averaged. Lowerpanel: 28-day averages based on Aanderaa current meters moored over the mid-channel hump (Mooring 3) and ADP observations in the flood (western) channel, where the contour interval equals 1 cm/sec. Note that in each panel, the zero-speed contour or line of no-net-motion lies over the mid-channel hump.

For comparison with the hydrodynamical model, water flow into the inlet was expressed in discharge units known as volume transport. Net north-south current speeds derived ADP profiles were averaged for integer numbers of 28 days within a five-month period and contoured along transects across the outer and central inlets (Figure 6). Net volume transports of the inflows and outflows were then estimated from the contours (Table 2). Volume transports computed from the measurements and hydrodynamic model differed to a small degree (3–12%).

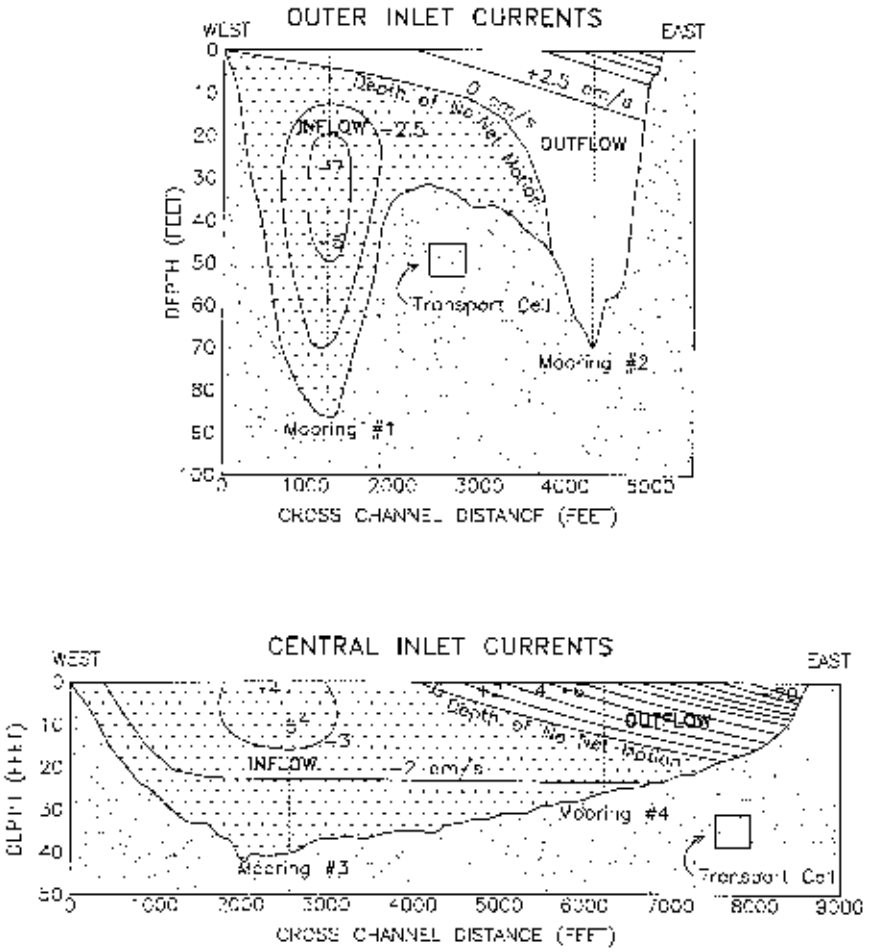

Figure 6. Current speed across Budd Inlet: currents during the hydrodynamical model runs. Top panel: outer inlet contours are based ADP observations at sites (Moorings) 1 and 2 on the west and east tidal channels, respectively. Bottom panel: Central inlet contours are based on sites 3 and 4 on the west and east sides of the channel, respectively. Northward transport was computed for the region of the cross section having positive speeds, and southward transport for the area of negative speeds (stippled). No net north-south motion occurs along the zero-speed contours. Transport cells represent the cross sectional unit areas in which transport was computed; these were summed to obtain the overall transport.

The north-south speed contours show the major features of the tidally averaged flow (Figures 5, 6). In the outer inlet a submerged core of higher velocity heads southward along the western shore, and a shallow plume of higher velocity moves northward along the eastern shore (Figure 6, upper panel). A similar pattern occurs in the central inlet, except that the western core of high velocity may extend to the sea surface, and the high-velocity outflowing layer is deeper and wider along the eastern shore (Figure 6, lower panel).

Table 2. Transports in Budd Inlet's inflowing and outflowing layers computed from current measurements and the hydrodynamic model. The current measurements were averaged during November 1996 through April 1997; hydrodynamic model results apply to 6 November 1996 through 31 January 1997. ***, the outflowing layer was too shallow to be sampled by the ADP at site 2 (see Figure 1 for locations).

Transect	**Water Transport (m^3/sec)**					
	South flow/ west shore			**North flow/ east shore**		
	Model	Meas.	% Difference	Model	Meas.	% Difference
Outer	-274	-281	3%	+315	***	
Central	-336	-352	5%	+374	+333	12%
Inner	-163	no data	---	+199	no data	---

Based on transports computed from the field data and the hydrodynamic model, schematic circulatory diagrams were constructed (Figures 7 and 8). For the volume transports associated with 16 or so elements of the flow patterns, see the captions in Figures 7 and 8. In general, approximately half of the outer inlet inflow reverses direction in the central inlet and exits via the outer inlet. Coriolis acceleration drives the inflows and outflows to the west and east sides of the inlet, respectively, augmenting the lateral flow separation. A secondary fraction recirculates in a gyre around the central inlet.

The forces driving the circulation were confirmed by the GLLVHT hydrodynamic and transport model. Figure 9 shows the model-computed circulation and surface salinities through a tidal cycle in the summer months. It shows on falling tide that there is still some inflow along the western side at the outer boundary and a gyre in the center of the inlet. As the tide falls, the currents become intensified along the eastern shore of the inlet. On a rising tide, the inflowing current is intensified along the western shore of the inlet

The modeled surface salinities in Figure 9 show that the low-salinity lens extending outward along the eastern shore on a falling tide produces a lateral distribution of salinity similar to that found from the data as shown in Figure 2 and Figure 3. The lateral distribution of salinity persists throughout the tidal cycle.

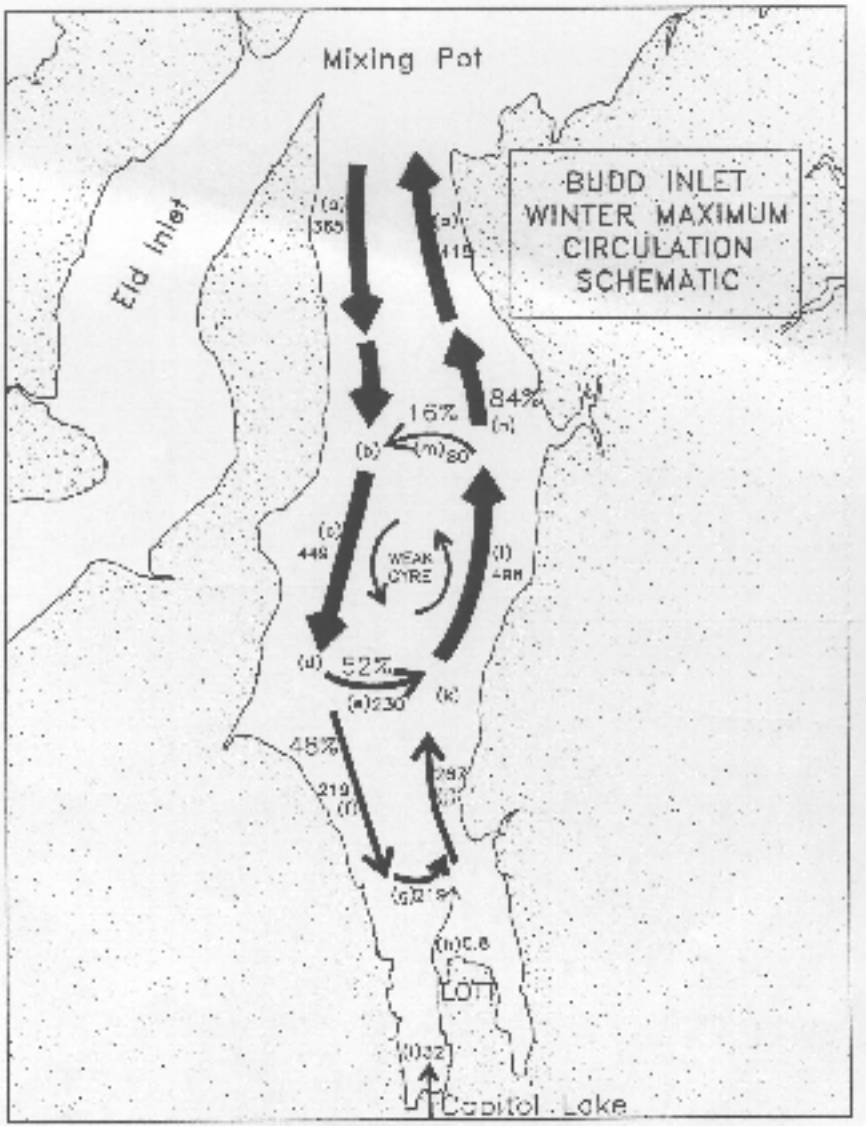

Figure 7. Plan view of Budd Inlet circulation during January 1997. The arrows indicate water flow scaled in thickness approximately proportionate with net volume transport (m^3/sec). Refluxing is shown by the percentages of the main flows diverted east and west across the inlet forming the weak gyre in the central inlet. Letter codes (a – o) following the water flow clockwise around the inlet denote the following: a) from the mixing pot the outer inlet main inflow transports southward 365 m^3/sec as a submerged jet-like current hugging the western shore of the outer inlet; (b) outer inlet main inflow merges with water refluxed from the outflow in the Central inlet; c) main inflow in the Central inlet equals 449 m^3/sec comprised of 82% water from the outer inlet (365 m^3/sec) and 18% water refluxed from the central inlet main outflow (80 m^3/sec); d, e) Central inlet main inflow diverges with approximately half (48%; 219 m^3/s) flowing into the inner inlet, and half refluxing (e; 52%; 230 m^3/sec) around the weak central inlet gyre; f) inner inlet main inflow (219 m^3/sec) moves southward to the vicinity of the LOTT outfall; g, h, i) inner inlet main inflow merges with discharges from LOTT (h) and Capitol Lake (i); j) inner inlet main outflow (267 m^3/sec) exits primarily as a thin (order of few meters thick) layer; k) inner inlet main outflow merges with water refluxed from the Central inlet main flow; l) Central inlet main outflow in a thin layer a few meters thick (498 m^3/sec) flows around the east side of the weak gyre; m, n) Central inlet main outflow diverges (n) with a secondary fraction (m; 16%; 80 m^3/sec) refluxing westward into the Central inlet main inflow (b, c); and (o) outer inlet main outflow (418 m^3/sec) exits northward to the mixing pot.

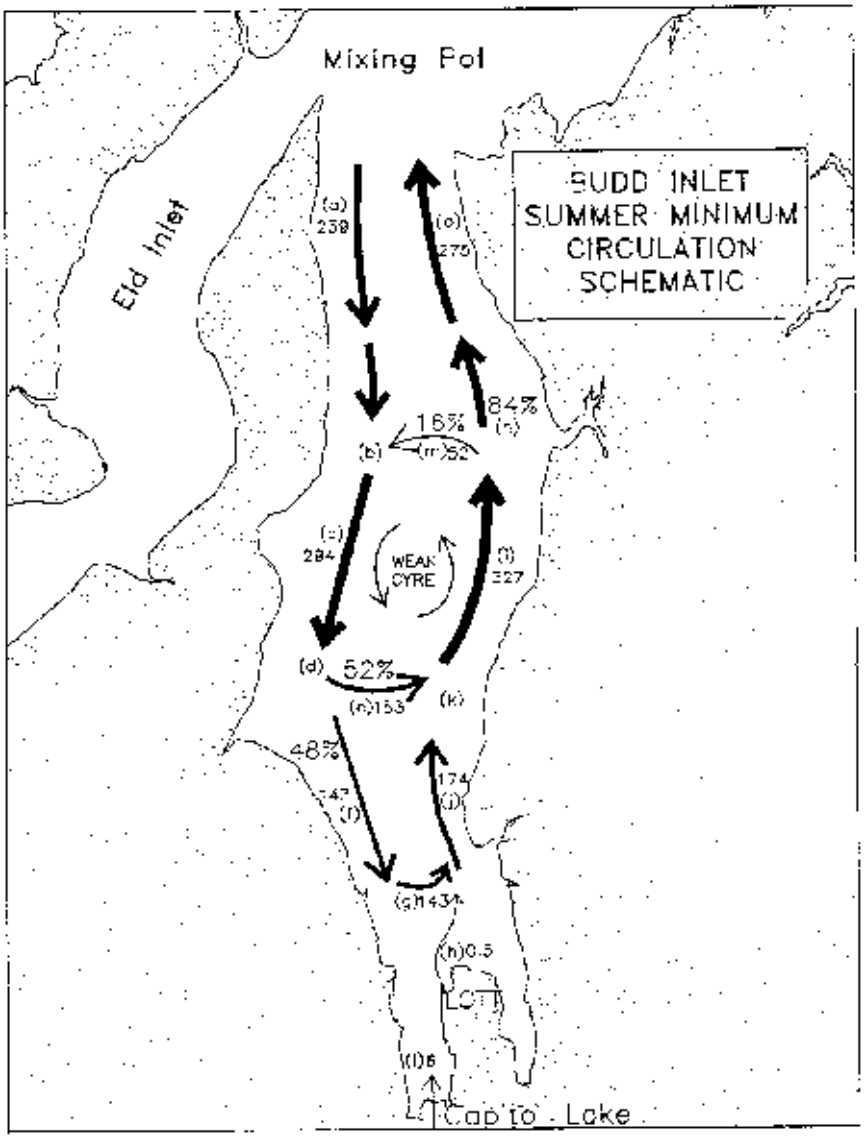

Figure 8. Plan view of Budd Inlet circulation during August 1997. The arrows indicate water flow scaled in thickness approximately proportionate with net volume transport (m^3/sec). Refluxing is shown by the percentages of the main flows diverted east and west across the inlet forming the weak gyre in the Central inlet. Letter codes (a – o) following the water flow clockwise around the inlet denote the following: a) from the mixing pot the outer inlet main inflow transports southward 239 m^3/sec as a submerged jet-like current hugging the western shore of the outer inlet; b) outer inlet main inflow merges with water refluxed from the outflow in the Central inlet; (c) main inflow in the central inlet equals 294 m^3/sec comprised of 82% water from the outer inlet (239 m^3/sec) and 18% water refluxed from the central inlet main outflow (52 m^3/sec); d, e) Central inlet main inflow diverges with approximately half (48%; 143 m^3/sec) flowing into the inner inlet, and half refluxing (e; 52%; 153 m^3/sec) around the weak central inlet gyre; f) inner inlet main inflow (143 m^3/sec) moves southward to the vicinity of the LOTT outfall; g, h, i) inner inlet main inflow merges with discharges from LOTT (h) and Capitol Lake (i); j) inner inlet main outflow (174 m^3/sec) exits primarily as a thin (order of few meters thick) layer; k) inner inlet main outflow merges with water refluxed from the Central inlet main flow; l) Central inlet main outflow in a thin layer a few meters thick (327 m^3/sec) flows around the east side of the weak gyre; (m, n) Central inlet main outflow diverges (n) with a secondary fraction (m; 16%; 52 m^3/sec) refluxing westward into the central inlet main inflow (b, c); and o) outer inlet main outflow (275 m^3/sec) exits northward to the mixing pot.

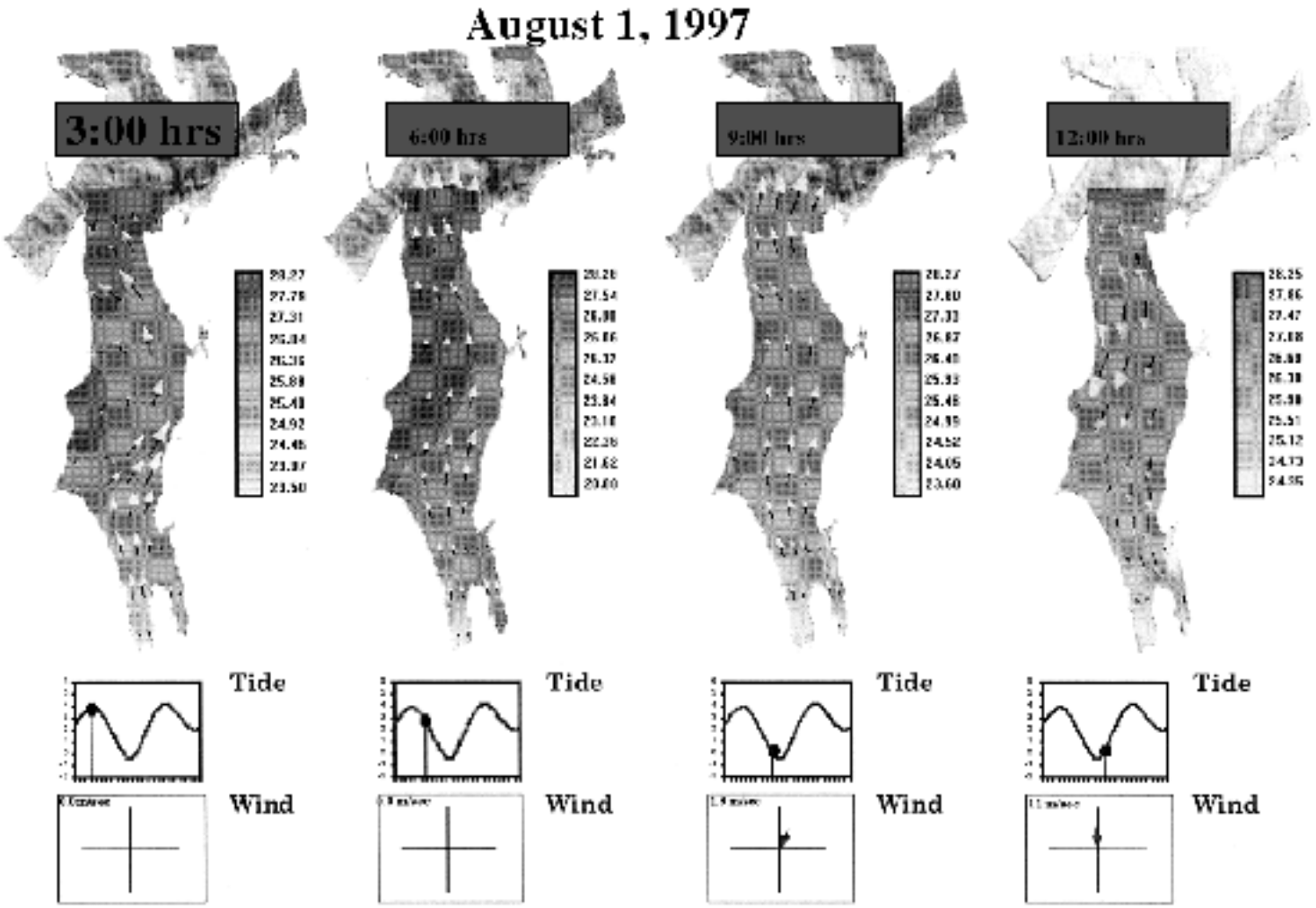

Figure 9. Surface velocities and salinity through a tidal cycle from the GLLVHT model. Time and tide proceed left to right as shown at top and bottom, respectively.

Results: Transport and Flushing

To evaluate how fast Puget Sound water enters the inlet, southward transport was computed from north-south speed contoured across flood tidal channel in the BE transect (e.g., Figure 5, lower panel). Eleven 28-day average ADP profiles were contoured assuming zero no-net-current at mid-channel (above the outer inlet mid-channel hump).

A regression fit to the 11 estimates of the estuarine volume transport (T) and Capitol Lake discharge (Q) data averaged for 28 days, yielded the following equation (Figure 10):

T	**=**	**222**	**+**	**3.61Q,**	**(1)**
Volume transport		**Tidal pumping**		**River effect**	

where: T= southward transport through the BE transect (m^3/sec); Q=Capitol Lake discharge (m^3/sec); *r*=correlation coefficient (0.861; and *n*=sample size (11).

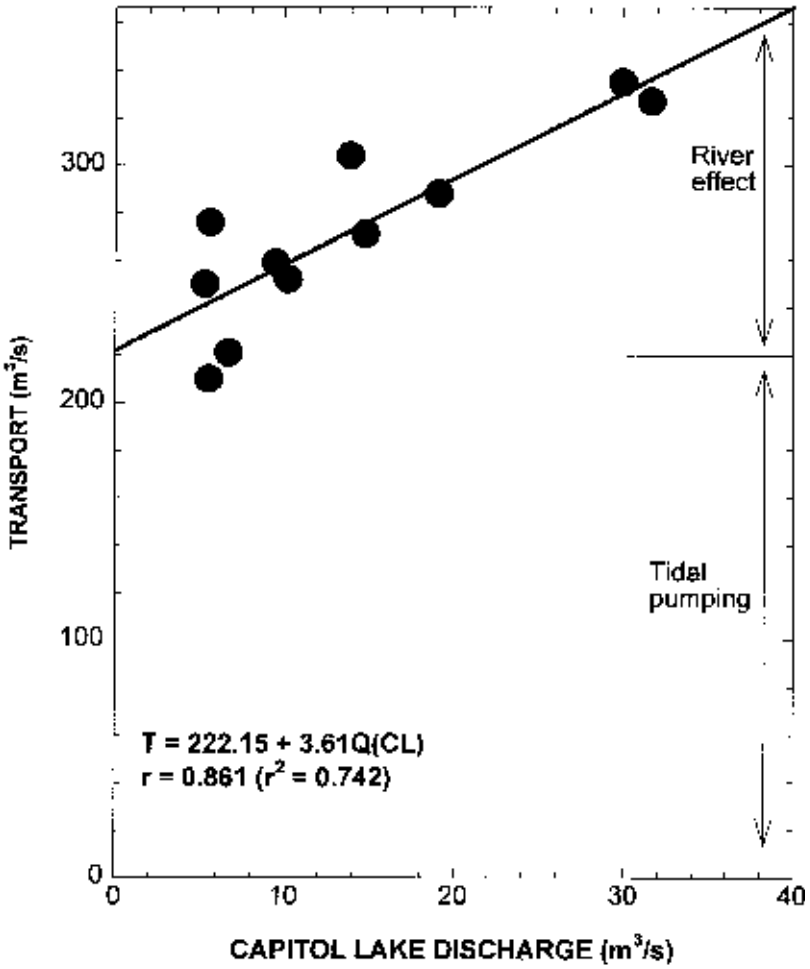

Figure 10. Estuarine transport versus Capitol Lake discharge. Dots represent 28-day average transports southward across the BE transect (see Figure 1 for location) and corresponding discharge from the Deschutes River via Capitol Lake. Equation and regression coefficient (r) represent the linear regression fit (see equation 1).

To evaluate whether the transports adequately represented a seasonal cycle, the inflowing currents measured at site 1 were further examined. First, 28-day average north-south speeds were displayed versus depth for the entire field year (Figure 11). Each profile showed southward flow from near the sea surface to the sea floor with maximum southward speed near a normalized depth of 0.6 m. Second, the north-south currents at the maximum inflow depth (~8m) depth were filtered with running tidal day and 28-day filters (Figure 12, upper panel). It can be seen that the daily values vary through a well-behaved seasonal cycle and the 11 transport estimates capture the extremes of this cycle.

Flushing (F) was estimated as the time for the net inflowing transport to replace the inlet's volume at MHHW, or F = [230,000,000/(222 + 3.61 Q)]/86,400 days, F = 2,662/(222 + 3.61Q) days. Values of F for the field year fluctuated from about 7 days in winter to 11 days in summer.

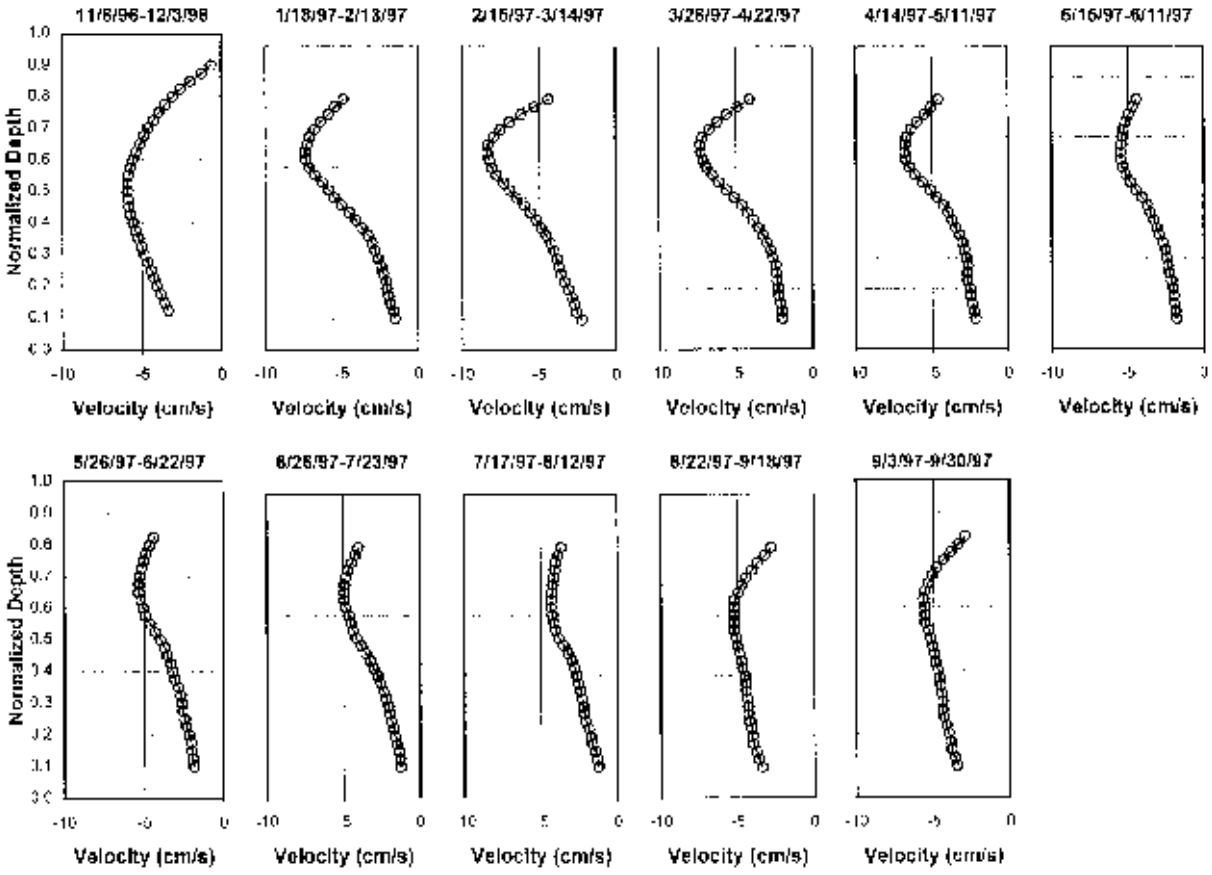

Figure 11. Vertical profiles of 28-day average north-south current speed at site 1. These 11 profiles were used to compute the volume transports (11 panels, left to right, top to bottom; see Figure 1 for mooring location). The 28-day average profiles begin in November 1996 and continue through September 1997.

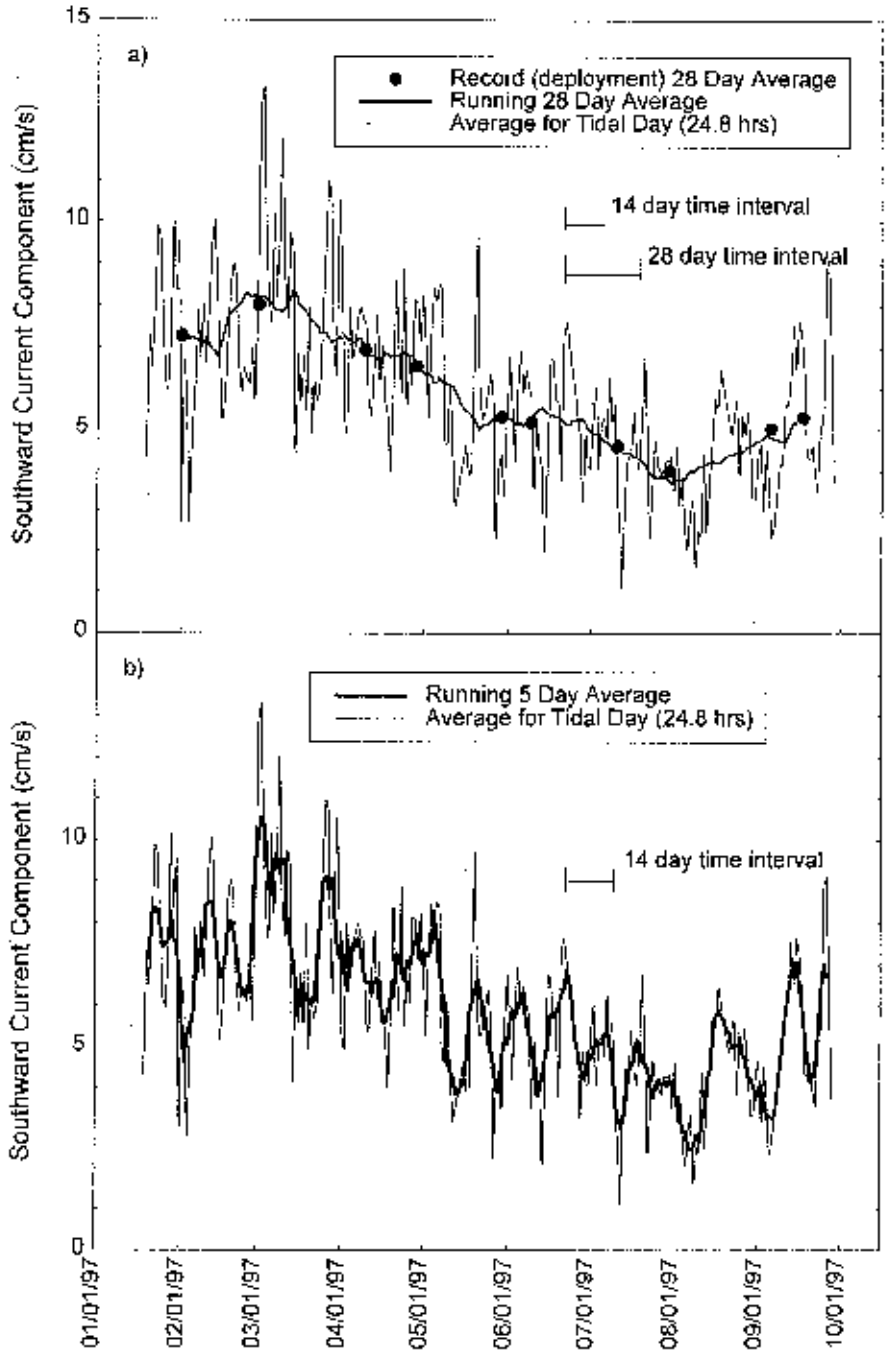

Figure 12. Seasonal cycle of maximum inflowing currents at site 1. In both panels the lighter solid line was obtained by averaging the ADP data at 8-m depth over 24.84-hour intervals. Top panel: heavier solid line, 28-day running average of the daily values; heavy dots, the mid-points of the 28-day intervals during which volume transports were calculated along the BE transect (see Figure 1). Bottom panel: heavier solid, 5-day boxcar running average of the daily values.

Tidal Pumping

The regression coefficient for equation (1) indicates that Capitol Lake discharge explains 74 percent of the outer inlet transport variance. Since Capitol Lake discharge during the field year fluctuated by approximately 35 m^3/sec, the addition of fresh water to the inlet explains approximately 126 m^3/sec of the outer inlet's transport compared with the much larger constant transport of 222 m^3/sec in equation (1). Furthermore, to preserve continuity within the inlet, a physical mechanism must lift the inlet's thick, deep inflow into its shallow outflowing layer. Therefore, we searched for a physical mechanism that upwelled water at the inlet's head at a rate equal to the constant in equation (1).

Several factors suggested tidal dynamics as the upwelling mechanism:

1. Tidal dynamics within Puget Sound are well known to undergo pronounced variations at two-week intervals. Power spectra of the daily net north-south speeds at site 1 showed a significant peak at a period of two-weeks (Dr. Robert J. Stewart, personal communication). In the time-series of daily net speeds smoothed with a five-day running average, the speed maxima are separated by an average of two weeks (Figure 12, lower panel).
2. The shape of the sea floor and the intertidal volumes suggested a tidal mechanism. On the western side of the inlet, the 18-foot depth contour intrudes southward forming an upwelling channel for the flooding currents. On the eastern side, the outflowing layer is underlain by shallower depths deposited from Capitol Lake discharges that rain sedimentary materials downward from the outflowing layer.
3. The volume of water between high and low tides increases markedly toward the head of the inlet (Table 3). For the entire inlet the volume between Mean-Higher-High Water (MHHW) and Mean-Lower-Low Water (MLLW), taken as the tidal prism, approximately equals the volume below MLLW (ratio in Table 3). Southward, the ratio increases dramatically, reaching 2.72 in the inner inlet. On the average each day, the tide drains approximately 73% of the inner inlet's volume at the tide's highest stand.

Table 3. Water volumes within Budd Inlet segments below high and low tides. Notation: MLLW, mean lower low water; MHHW, mean higher high water.

	Volume (10^6 m^3)			
Inlet Segment	MHHW (1)	MLLW (2)	MHHW-MLLW (3)	RATIO (3)/(2)
Entire inlet	230.1	119.0	111.1	0.93
Central + Inner	131.1	60.0	71.1	1.19
Inner	35.4	9.52	25.88	2.72

The transport associated with the tides may be computed as follows. Assume that the tidal prism of the inner inlet fills on flood tides with water from the inflowing layer and subsequently drains into the inlet's outflowing layer. Taking the intertidal volume between the average highest daily stand of the tide and the average lowest tide (i.e., between MHHW and MLLW; Table 3), divided by the length of a tidal day, yields 289 m^3/sec. Uncertainties in the tidally-derived transport arise because the boundary for the inner inlet is imprecise, and some ebb water undoubtedly returns (refluxes) on flood tides to the inner inlet.

While evaluating the flushing potential of the inner inlet, Albertson et al. (1998) estimated the upwelling where URS (1986) previously noted upwelling in contours of ammonium, nitrate, and nitrite. Using simplified box models and environmental data (Capitol Lake discharge, inlet salinities) for spring through fall of three years (1992, 1993, 1994), Albertson et al. (1998) estimated an annual average upwelling transport of 313 m^3/sec.

Despite the uncertainties, the agreement of the tidal pumping estimate with those from measured currents and the box and hydrodynamic models points to tidal pumping, which rapidly uplifts and transfers water from the inlet's inflowing to its outflowing layer.

Discussion

Computers and hydrodynamic modeling have evolved rapidly in the past few years. Three-dimensional models with fine spatial meshes and small time steps are now routinely applied to estuarine circulation. Distilling this body of experience, Jian Wu et al. (1998) write: "One fundamental principle that has been learned is that the water quality within a water body can only be modeled to the detail with which the hydrodynamics of that water body is known." Careful 3-D modeling of Budd Inlet has clearly verified the lateral separation of the inlet's inflowing and outflowing currents as observed with the current meters.

Lacking a 3-D model and comprehensive current measurements, previous studies estimated water transport in the inlet by applying laterally-averaged box models to hydrologic (river discharge) and hydrographic (salinity) data. Because the previous data were collected mostly at mid-channel or did not adequately represent the laterally separated flow layers, the resulting transports varied widely up to 2,000 m^3/sec compared with the present estimate of approximately 300 m^3/sec (URS Corporation, 1986).

The present results suggest that tidal pumping maintains a vigorous circulation year-round in Budd Inlet, secondarily controlled by discharge from Capitol Lake. Water properties (temperature, salinity, density, oxygen), reflecting the pump, change primarily across the inlet rather than down inlet as is typical of estuaries because the pump draws water from one side of the inlet and expels it along the other side.

Acknowledgements

This study was funded by the LOTT Partnership (Lacey, Olympia, Tumwater, Thurston County). We thank: Charles D. Boatman, AuraNova Consultants, and Skip Albertson, Washington Department of Ecology, for many helpful comments; Matt Davis, Brown and Caldwell, Inc., for computing the vertically averaged profiles; Robert Stewart, Digital Analogics, Inc., for computing current power spectra; Brent Johnston, Northwest Aerial Reconnaissance, Inc. for contouring the water properties; Clay Wilson for calibrating the CTD sensors; Tim Crone, Evans-Hamilton, Inc., making the illustrations; and Keith Kurrus and Eric Noah, Evans-Hamilton, Inc., for servicing the current meter moorings.

References

Albertson, Skip, M. Edie, and M. Davis. 1998. Seasonal and interannual variations of residence (flushing) time in the west bay of Budd Inlet. Proceedings of the Puget Sound Research Conference held 12–13 March 1998 in Seattle. Puget Sound Water Quality Action Team, Olympia, Washington.

Davis, M., C. Coomes, C. Cleveland, and C. Ebbesmeyer. 1998. Inlet hydrodynamics under a highly varying, non-steady discharge: Capitol Lake and its impact upon Budd Inlet. Proceedings of the Puget Sound Research Conference held 12–13 March 1998 in Seattle. Puget Sound Water Quality Action Team, Olympia, Washington.

Edinger, J.E. and E.M. Buchak. 1995. Numerical intermediate and far field dilution modelling. Water, Air and Soil Pollution 83: 147–160. Kluwer Academic Publishers.

McLellan, P.M. 1954. An area and volume study of Puget Sound, Washington. Univ. of Washington, Department of Oceanography Techncial Report No. 21., Feb. 1954.

URS Corporation. 1986. Comprehensive circulation and water quality study of Budd Inlet. Final report, Southern Puget Sound water quality assessment study, submitted to Washington Department of Ecology July 31, 1986.

Wu, J., V. S. Kolluru, and J. E. Edinger. 1998. Combined hydrodynamic and water quality modelling for waste water impact studies. Proceedings of Mid-Atlantic Industrial Wastes Conference, Lee Christensen ed., Villanova University, July, 1998.